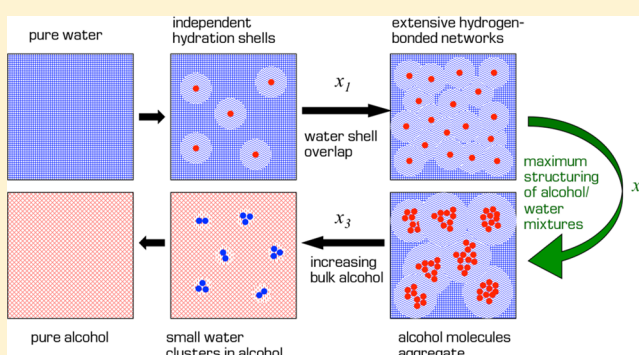Article

Mesoscopic Structuring and Dynamics of Alcohol/Water Solutions Probed by Terahertz Time-Domain Spectroscopy and Pulsed Field Gradient Nuclear Magnetic Resonance

Ruoyu Li, Carmine D'Agostino, James McGregor,[†] Michael D. Mantle, J. Axel Zeitler,* and Lynn F. Gladden*

Department of Chemical Engineering and Biotechnology, University of Cambridge, Pembroke Street, Cambridge, CB2 3RA, United Kingdom

S *Supporting Information*

ABSTRACT: Terahertz and PFG-NMR techniques are used to explore transitions in the structuring of binary alcohol/water mixtures. Three critical alcohol mole fractions (x_1, x_2, x_3) are identified: methanol (10, 30, 70 mol %), ethanol (7, 15, 60 mol %), 1-propanol (2, 10, 50 mol %), and 2-propanol (2, 10, 50 mol %). Above compositions of x_1 no isolated alcohol molecules exist, and below x_1 the formation of large hydration shells around the hydrophobic moieties of the alcohol is favored. The maximum number of water molecules, N_0, in the hydration shell surrounding a single alcohol molecule increases with the length of the carbon chain of the alcohol. At x_2 the greatest nonideality of the liquid structure exists with the formation of extended hydrogen bonded networks between alcohol and water molecules. The terahertz data show the maximum absorption relative to that predicted for an ideal mixture at that composition, while the PFG-NMR data exhibit a minimum in the alkyl chain self-diffusivity at x_2, showing that the alcohol has reached a minimum in diffusion when this extended alcohol−water network has reached the highest degree of structuring. At x_3 an equivalence of the alkyl and alcohol hydroxyl diffusion coefficients is determined by PFG-NMR, suggesting that the molecular mobility of the alcohol molecules becomes independent of that of the water molecules.

INTRODUCTION

The structure and dynamics of mixtures of water and a hydrophobic or amphiphilic solute have been widely studied over the past eight decades. Such solutions play an important role in many biological, chemical, and engineering applications; examples include protein folding, membrane self-assembly, electron transfer reactions, heterogeneous catalysis, and fuel cell technology.[1−4] Despite this, however, the influence of the solute molecules upon the structure of water is not yet fully understood.[3] Early studies explained the larger than expected decreases in entropy and enthalpy upon mixing by suggesting an enhancement in the structuring of water molecules in the hydration shell of the solute molecule, that is, the water structure becomes more ice-like.[5] More recent studies have proposed alternative explanations for such observations. For instance, neutron diffraction studies do not show an enhancement in the structuring of hydration water and suggest that the anomalous properties upon dissolution arise from incomplete mixing on the molecular level,[6,7] while femtosecond infrared (fs-IR) spectroscopy measurements confirm that the "iceberg" model cannot fully explain the suite of experimental data that now exists.[8] The latter study proposes an alternative entropic origin. Specifically, the presence of hydrophobic moieties

sterically hinders the formation of the five coordinated water molecules, which have been shown to be responsible for the high rotational mobility of water.[9] In the absence of five-coordinated molecules the rotational and translation dynamics of water are retarded. At present, a clear consensus on the origin of the anomalous physical properties of such solutions has not yet been reached, with dynamical and structural measurements often yielding apparently contradictory results. The chemically most simple aqueous amphiphile solutions, alcohol/water mixtures, have received much attention and have been investigated by a range of experimental techniques including neutron diffraction,[6,7] NMR,[10−12] Raman spectroscopy,[13,14] infrared spectroscopy,[8,15] dielectric spectroscopy,[16] and mass spectrometry,[17] as well as numerical and computational studies.[18,19] Generally, such studies identify one or more transitions in the structure of alcohol/water mixtures. Taking aqueous ethanol as a representative example, excess enthalpy, heat capacity, diffusivity, and viscosity all exhibit maxima or minima at ∼15−20 mol %;[12,16,20−23] this is attributable to

changes in the hydrogen-bonding interactions in the mixture. Raman spectroscopy has also shown a transition at ~7 mol %, attributed to the concentration at which individual ethanol molecules are no longer coordinated by water molecules alone.[22] Recent studies on glycerol have demonstrated the importance of understanding the extended hydrogen-bonding network in such systems rather than focusing solely on the local water structure.[24,25] In order to gain insight into the structuring of aqueous alcohols, and transitions in their structure as a function of composition, it is necessary to employ experimental techniques that probe dynamical processes within extended hydrogen-bonded networks.

Terahertz time-domain spectroscopy (THz-TDS) is a spectroscopic technique that is able to probe the rotational and vibrational dynamics of molecules in the frequency range between 100 GHz and 4 THz.[26,27] It covers parts of the far-infrared region of the electromagnetic spectrum and probes molecular motions dominated by intermolecular interactions, in particular, hydrogen bonds.[28−31] In contrast to crystalline materials, where well-defined terahertz absorption peaks are observed due to the long-range order present in such systems,[32−34] the terahertz absorption spectra of liquids are well-known not to exhibit any such distinctive absorption bands.[35−37] Due to the ability to measure amplitude and phase of the transmitted waveform in THz-TDS, complex dielectric spectra of alcohol/water mixtures in the terahertz range can be calculated directly from the experimental data.[38−42] Dielectric relaxation analysis can then be applied to yield information on the structure and rotational dynamics of the liquids.

In general, the dielectric spectra of polar liquids start at zero frequency (static dielectric constant) and exhibit their main peaks at microwave frequencies, the high frequency wings of which extend into the terahertz range. The spectra are the result of reorientational motions of polar molecules excited by an external oscillating electric field, e.g. the terahertz radiation in the case of THz-TDS. Therefore, the dielectric spectrum represents the rotational dynamics of liquid molecules. To date, a significant amount of work has been reported on studying the microwave dielectric spectra of alcohol/water mixtures at GHz frequencies.[43−53] Barthel et al.[43] found that in the liquid state the microwave dielectric spectra of lower members of aliphatic alcohols consist of three distinct relaxation processes with decreasing characteristic relaxation times that are assigned to cooperative rearrangement of the alcohol−alcohol chain structure (~100 ps), reorientation of a monomer situated at the end of the alcohol−alcohol chain (~10 ps), and liquid molecules in the process of hydrogen bond formation and decomposition (~1 ps).[43,54] With the advent of THz-TDS, there has been a strong interest in extending dielectric spectroscopy to the terahertz range. The Debye model, which has proved to be useful in studying dielectric relaxation phenomena at microwave frequencies,[45−53] remains valid in the terahertz frequency range, and is widely used in the study of liquids.[55−58] The temperature dependence of dielectric relaxation processes in liquid water has been studied and the origins of different relaxation components have been discussed with the aid of molecular dynamics (MD) simulations and studies on deuterated water.[55−59] The hydration shells formed around dissolved protons in water have been reported by Tielrooij et al.[57] In particular, terahertz spectroscopy has been used in combination with infrared and MD simulations to study the structure of methanol/water mixtures[58] and acetonitrile/water mixtures.[60] In a recent paper by Tielrooij et al.,[61] the

dielectric response of tetramethylurea was measured using a combination of terahertz and gigahertz dielectric spectroscopy and the results were compared to femtosecond infrared pump−probe studies. By investigating a range of concentrations of aqueous tetramethylurea solutions it was found that the dynamics of the water molecules in close vicinity to the hydrophobic urea derivative was significantly slowed down but that this effect did not extend further than approximately 12 water molecules into the bulk water phase.

In the present study ^{1}H NMR spectroscopy is used to complement the THz-TDS analysis. The ^{1}H NMR spectra of alcohol/water mixtures have been reported with increasing accuracy in a number of studies.[12,62−65] A shift of the water ^{1}H peak to lower magnetic field in the water-rich region of ethanol/water mixtures was observed and this was attributed to the strengthening of hydrogen bonds between water molecules.[63] The separation between the water ^{1}H peak and the hydroxyl ^{1}H peak of the ethanol molecule at higher ethanol concentrations was explained by the formation of ethanol−ethanol clusters in the mixture.[62] In addition to the spectral analysis the ^{1}H NMR spin−lattice relaxation time (T_1) of water molecules was measured for a range of alcohol/water mixtures.[66,67] An inflection point of the T_1 values was found in different alcohol/water mixtures, which implies a transition in the liquid structure from the water dominated region to the alcohol dominated region.[67] Moreover, pulsed-field gradient nuclear magnetic resonance (PFG-NMR) has been used to determine the self-diffusion coefficients (D) of molecules in the mixtures of methanol/water and ethanol/water, and *tert*-butyl alcohol/water.[68] It was found that D changes with the composition of the mixture and that this change correlates with the hydrogen bonded network formed within the mixtures. Based on these studies it was concluded that *tert*-butyl alcohol had the greatest ability to stabilize water through hydrophobic hydration. Further, the results provided evidence for alcohol self-association in very dilute solution; this effect again being greatest for *tert*-butyl alcohol.

In this study we apply THz-TDS and PFG-NMR to systematically study the structure of alcohol/water mixtures. We specifically investigate hydrogen bonded alcohol/water networks that form in the mixtures of methanol/water, ethanol/water, 1-propanol/water, and 2-propanol/water. For the analysis of the terahertz data, we have used a combination of different analysis techniques that we have validated using the PFG-NMR data. We demonstrate that the use of terahertz spectroscopy in combination with PFG-NMR provides a powerful approach to studying both the structure and dynamics of these binary liquid mixtures.

■ EXPERIMENTAL METHODS

Samples. Aqueous solutions of a series of simple aliphatic alcohols were studied by mixing deionized water (50 mΩ) with the appropriate amounts of methanol (>99.5%, Fisher Scientific), ethanol (>99.8%, Fisher Scientific), 2-propanol (>99.8%, Fisher Scientific), or 1-propanol (>99.7%, Sigma-Aldrich).

Terahertz Time-Domain Spectroscopy. The THz-TDS transmission setup used in this study has been described previously.[32] The liquid samples were contained within a liquid cell (PIKE Technologies, Madison U.S.A.) contained between 3 mm thick z-cut quartz windows, which are transparent to terahertz radiation, separated by a 200 μm thick PTFE spacer. The sample liquid was injected through two holes drilled into

the quartz window. For each sample, 200 time-domain waveforms were collected (3 min acquisition time), averaged, and then transformed into the frequency domain by fast Fourier transformation (FFT). Due to the large optical mismatch between the quartz/air and quartz/sample interfaces, multiple non-negligible internal reflection pulses from the quartz window were detected. Therefore, a cutoff time before the first reflection pulse (~43 ps) was selected prior to the FFT to eliminate any etaloning artifacts due to these multiple reflections. All samples were measured at 293 ± 1 K. A sample cell with no spacer was used for the reference measurement. Data were acquired in the frequency range 0.2–2.0 THz, similar to that reported by Venables and Schmuttenmaer in their studies of mixtures of acetone, acetonitrile and methanol with water.[58,60] The terahertz absorption spectra were calculated using the Beer–Lambert law from the acquired data by truncating the waveforms 20 ps after the main peak which is just before the first etalon reflection from the quartz windows.

In order to extract the complex dielectric constant, we use the solution derived by Duvillaret et al.[38] to account for all losses due to the multiple reflections between the quartz window and sample interface (Figure 1):

$$\tilde{E}_{\text{transmitted}} = \tilde{E}_{\text{ref}} T_{qs} T_{sq} P_s \left[\sum_{\infty}^{j=0} (R_{qs}^2 P_s^2)^j \right] \tag{1}$$
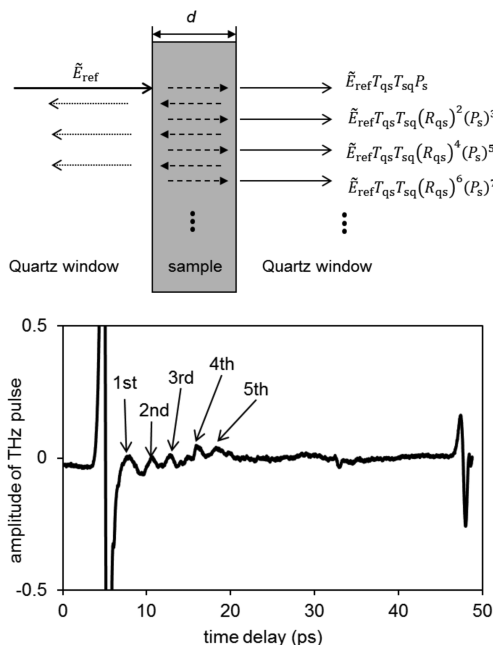

Figure 1. Single-slab model of terahertz radiation propagating through the liquid cell (top). Identification of echo pulses originating from the multiple reflections within the sample layer (bottom).

where T_{qs}, T_{sq}, and R_{qs} are the Fresnel coefficients and $P_s = \exp[-(i w n_{\text{sam}} d)/(c_0)]$ is the propagation term (n_{sam} is the refractive index of the sample, d is the thickness of the sample, c_0 is the speed of light, ω is the frequency, and $n_{\text{quartz}} = 2.12$).

The time-domain waveform was truncated at 40 ps before the first echo pulse due to the interface the between quartz window and air is observed (Figure 1). For a sample layer of 200 μm thickness with an estimated refractive index of 2.5, this truncated time-domain waveform includes about 12 echo pulses

between the quartz windows and the sample interface. Careful analysis of the time-domain waveform reveals that only the first five echo pulses are detectable within this 40 ps window: due to the strong absorption subsequent echo pulses from the sample layer are attenuated below noise level after 20 ps, and hence, it is justified to use the solution derived by Duvillaret et al.[38] for an infinite number of multireflections to extract the complex dielectric constant measured in this study even though our waveforms are truncated to 40 ps.

Pulsed Field Gradient Nuclear Magnetic Resonance (PFG-NMR). ^{1}H NMR spectra of different alcohol/water mixtures were acquired at 293 ± 1 K. All NMR measurements were conducted using a Diff-30 diffusion probe with a 10 mm radio frequency coil on a Bruker DMX 300 spectrometer, operating at a ^{1}H resonance frequency of 300.13 MHz. The chemical shifts are quoted using the ^{1}H resonance of tetramethylsilane (TMS) as an external reference. PFG-NMR self-diffusion measurements were carried out using the PGSTE pulse sequence,[69] with 16 equally spaced gradient increments starting from the minimum values of 0.05 Tm^{-1}. The maximum gradient strength was determined experimentally (1.2–3.0 Tm^{-1} for different compositions of alcohol/water mixture) to ensure the signal from the last echo was comparable to the noise floor. The diffusion encoding time Δ was fixed to 50 ms, while the gradient pulse duration δ was set to 1 ms. For all samples, 5 mm Wilmad NMR tubes were used, which were sealed during the measurement to prevent evaporation of solvent. A total of 16 signal averages were acquired for each gradient increment g, for a total of 16 increments, and the recycle time was 5 s, leading to a total acquisition time for an individual PFG-NMR data set of 21 min. In the water-rich region of some of the alcohol/water mixtures, the diffusion coefficient of the hydroxyl group is substantially biased by ^{1}H exchange between alcohol and water molecules.[64,68,70] In such cases, the self-diffusivity of water was calculated according to the method reported by Price et al.[68]

The area Ψ of respective resonance peaks was measured as a function of the gradient strength g and the self-diffusion coefficient D was then determined using eq 2.

$$\Psi = \exp\left[-\gamma^2 \delta^2 g^2 \left(\Delta - \frac{\delta}{3} \right) D \right] \tag{2}$$

where γ is the gyromagnetic ratio of the ^{1}H nucleus. The error in the self-diffusion coefficients are approximately 2% in all cases.

■ RESULTS

Terahertz Absorption Spectra. The terahertz absorption spectra of the pure liquids are plotted in Figure 2. The absorption spectra of alcohol/water mixtures are typical of those of pure liquids, which increase monotonically with frequency, and, as the relative amount of highly absorbing water is reduced, their overall absorption decreases as the alcohol mole fraction increases.

Using a simple volume mixing model the expected relative terahertz absorption coefficients at different concentrations can be calculated according to the following equations:

$$\alpha_{\text{ideal}}(\omega) = V_1 \alpha_1(\omega) + V_2 \alpha_2(\omega) \tag{3}$$

with

$$\alpha_{\text{relative}} = \alpha_{\text{ideal}} - \alpha_{\text{real}} \tag{4}$$
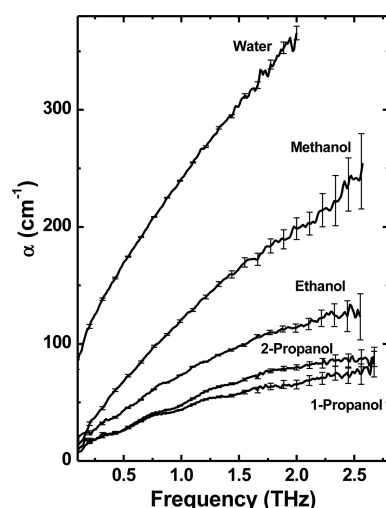
Figure 2. Terahertz absorption spectra of pure water and alcohols. The spectra of the alcohol/water mixtures are shown in the Supporting Information.

where V_1 and V_2 are the volume fractions of the pure liquids and α_1 and α_2 are their respective absorption coefficients at a selected frequency. α_{real} is the terahertz absorption coefficient of the alcohol/water mixture measured experimentally at the same frequency. For each alcohol concentration, the relative absorption coefficients were calculated at 0.5, 1.0, and 1.5 THz, respectively, and the average value calculated; the data are shown in Figure 2. The reason for plotting the average value of the absorption coefficient at three frequencies spanning the accessible bandwidth was to represent the overall terahertz response better than artificially choosing an arbitrary frequency. We found that changing the composition does not alter the general shape of the spectral response significantly.

Positive values of $\alpha_{relative}$ are obtained over the entire concentration range, indicative of a decrease of terahertz absorption upon mixing compared to the ideal mixture. These observations are consistent with those of Venables and Schmuttenmaer in their studies of acetone, acetonitrile and methanol with water,[58,60] and are interpreted as the addition of guest molecules disrupting the original hydrogen bonding structures that are present in the pure liquids to form a new hydrogen bonded alcohol/water network, which is characterized by slower rotational dynamics compared to the constituent pure liquids. In the present work, this maximum in the relative absorption data occurs at approximately 30, 15, 10, and 10 mol % for the mixtures of water with methanol, ethanol, 1-propanol, and 2-propanol, respectively.

The spectra of the mixtures can be related to the dynamical behavior of the liquids through the complex-valued dielectric constant, $\varepsilon_{Debye} = \varepsilon' - i\varepsilon''$. In recent years, many Debye-type models have been used to interpret terahertz and microwave frequency range data. In the interpretation of the data presented here we will use both the two-component[55,58,60] (eq 5) and three-component[43,54] (eq 6) Debye models:

$$\varepsilon_{Debye} = \varepsilon_\infty + \frac{\varepsilon_1}{1 + i\omega\tau_1} + \frac{\varepsilon_2}{1 + i\omega\tau_2} \tag{5}$$

$$\varepsilon_{Debye} = \varepsilon_\infty + \frac{\varepsilon_1}{1 + i\omega\tau_1} + \frac{\varepsilon_2}{1 + i\omega\tau_2} + \frac{\varepsilon_3}{1 + i\omega\tau_3} \tag{6}$$

where ω denotes the angular frequency and ε_∞ is the optical dielectric constant; ε_i and τ_i are the relaxation strength and dielectric relaxation time of the jth Debye relaxation component.; ε_i are considered as being equivalent to a population of a given mode, although the scaling constant relating the particular value of ε_i to a population need not be constant for different modes exiting within a single system. The assumption that the relaxation strength is directly proportional to the number of corresponding liquid molecules has been widely applied in the study of water content in soft matter[71,72] and in studies of the dynamics of aqueous mixtures.[57,73] The two-component model has been used by Venables and Schmuttenmaer in their studies of aqueous alcohol mixtures.[58,60] For completeness, we note the other Debye models that have been employed recently: the Havriliak–Negami model and related models employed by Sato and co-workers[45–53] and the model employed by Tanaka and co-workers[59] which includes one component for the intermolecular stretching vibration and one component for intermolecular libration, in addition to the slow and fast relaxation component of the two-component Debye model.

Consistent with the previously reported analysis of Venables and Schmuttenmaer it was found that the two-component Debye model provided the best fit to the pure, single-component alcohol data; fits were obtained to within the accuracy of the experimental data with the least number of fitting variables. We also note that while the use of the Debye model to fit terahertz data is widely accepted, it is important to recognize that the terahertz data cover a relatively small range of frequency to which to fit the data. The considerations in fitting the Debye model to this limited range of frequency data are now considered in the light of the subsequent analysis that will be performed.

Figure 4 shows the fits to the real and imaginary components of the dielectric spectrum of 2-propanol. The experimental data
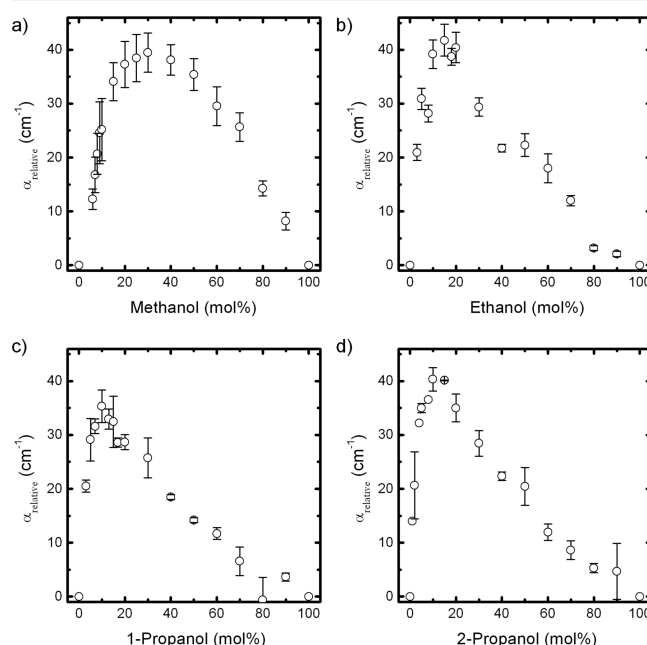

Figure 3. Relative terahertz absorption coefficients for different alcohol/water mixtures: (a) methanol/water, (b) ethanol/water, (c) 1-propanol/water, and (d) 2-propanol/water. For each data point, $\alpha_{relative}$ is the average of the relative absorption at 0.5, 1.0, and 1.5 THz.
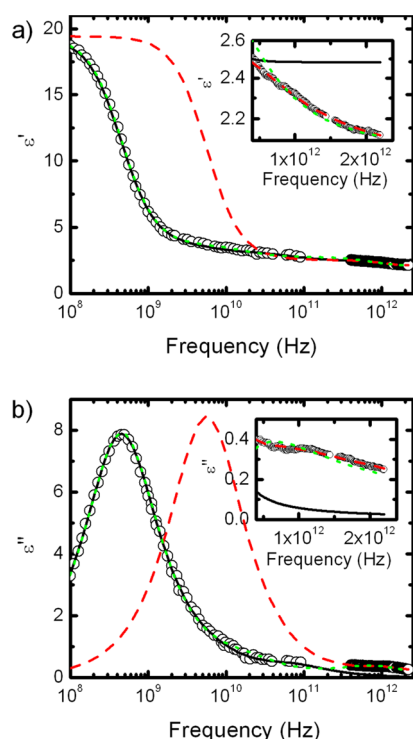
Figure 4. Fits of the Debye model to microwave (i.e., gigahertz) and terahertz data for 2-propanol: (a) real and (b) imaginary component of the dielectric spectrum. The experimental data are shown by the empty circles; the terahertz data are those acquired in the present work. The microwave data are those reported by Sato and Buchner.[48] Three fits are shown: (i) a three-component fit of the combined microwave and terahertz spectrum (green dotted line); (ii) a three-component fit to the microwave data alone (black solid line); (iii) a two-component fit to the terahertz data only (red dashed line).

are shown by the empty circles; the terahertz data are those acquired in the present work. The microwave data are those reported by Sato and Buchner.[45]

Three fits are shown in Figure 4: (i) a three-component fit of the combined microwave and terahertz spectrum (dotted line);

(ii) a three-component fit to the microwave (i.e., gigahertz) data alone (solid line); (iii) a two-component fit to the terahertz data only (dashed line). The numerical values of the fitting parameters providing the best fit in each case are given in Table 1; data are reported for all four pure alcohols and water. Considering the data shown in Figure 4, it is clear that the two-component fit to the terahertz data alone does not fit the gigahertz data. Further, the values taken from the three-component fit to the gigahertz data do not provide a satisfactory fit to the terahertz data acquired in the present work; this is particularly obvious with respect to the imaginary component of the dielectric spectrum. However, a three-component fit does provide good agreement with the combined GHz-THz data set.

Considering the data in Table 1, we see the sensitivity of the fitting parameters to the nature of the Debye model used. To within the experimental error of the acquired terahertz data, the two-component Debye is sufficient to describe the pure alcohol data. This is not surprising given that the terahertz frequency range over which data are acquired does not extend to sufficiently low frequencies that it can discriminate between modes of relaxation times of more than 1 ps. The three-component models are required to fit the microwave data alone and the combined GHz-THz data sets; note that for water only two components are needed regardless of whether a two- or three-component model is used.

Comparing all five liquids, we see that the results of the three-component fit to the combined GHz-THz data qualitatively agree with the findings reported by Barthel et al. in the 1990s, where it was reported that the microwave dielectric spectra of lower members of aliphatic alcohols consist of three distinct relaxation processes with characteristic relaxation times that were respectively assigned to cooperative rearrangement of the alcohol−alcohol chain structure (∼100 ps), reorientation of a monomer situated at the end of the alcohol−alcohol chain (∼10 ps), and liquid molecules in the process of hydrogen bond formation and decomposition (∼1 ps).[43,54] As the size of the molecules increases, the reorientation of polar molecules becomes more difficult leading to slower relaxation times. In our present study we have determined

Table 1. Dielectric Parameters of Pure Liquids Obtained by Fitting the Debye Model to the Terahertz Dielectric Spectrum, Microwave Dielectric Spectrum, and the Combination of Both, as Described in the Text[a]

		ε_∞	ε_1	τ_1 (ps)	ε_2	τ_2 (ps)	ε_3	τ_3 (fs)
THz	water	3.09	73.25	7.39			2.02	108
	methanol	1.90	29.03	13.96			1.35	134
	ethanol	1.98	21.75	19.23			0.77	155
	1-propanol	2.04	17.81	35.79			0.45	138
	2-propanol	2.01	16.90	28.45			0.52	139
GHz	water[45]	3.96	72.15	8.32			2.14	390
	methanol[43]	2.79	18.90	51.5	5.91	7.09	4.90	1120
	ethanol[48]	2.60	19.94	164.9	0.74	10.4	1.19	1690
	1-propanol[43]	2.44	11.05	329	3.74	15.1	3.20	2040
	2-propanol[45]	2.48	15.68	354.6	0.55	23.4	0.63	2120
THz + GHz	water	3.35	72.72	8.17			2.29	169
	methanol	1.79	26.82	49.98	2.46	1.22	1.21	107
	ethanol	2.00	20.06	163.6	1.42	3.98	1.03	222
	1-propanol	2.07	16.69	320.5	0.97	8.15	0.57	202
	2-propanol	2.05	15.77	350.9	0.89	9.14	0.71	218

[a]The results of the second term in the terahertz model are presented in the column representing the third term of the respective three-component Debye model because the fit parameter is considered to describe the same characteristic of the system.

systematically shorter relaxation times compared to those reported by Barthel et al., in particular, for the two faster relaxation processes. This is due to the inclusion of terahertz data to the fit which improves our understanding of the faster relaxation processes: as shown in Figure 4; a three-component fit that combines the GHz-THz data reproduces the higher frequency spectra better compared to the three-component fit to the GHz data only.

In agreement with a number of previous papers,[58,60] only a single picosecond relaxation term for alcohols is identified when analyzing the terahertz range alone using the two-component Debye model. This single term represents the appropriately weighted sum of the two picosecond Debye components identified from the three-component fit to the combined GHz-THz data. Compared to the femtosecond relaxation component, which represents the fast process of hydrogen bond formation and decomposition, the weighted picosecond relaxation component that is identified using the terahertz data only represents the overall relaxation process of hydrogen bonded bulk alcohol structures and hence the characteristic relaxation time of bulk alcohol structures in the terahertz range.

We now consider the analysis of the terahertz data acquired for the aqueous alcohol mixtures. As previously noted, Venables and Schmuttenmaer,[58] analyzed a subset of the same systems using a two-component Debye model. The slower mode that was fitted to the spectra fell in the range of 10 to 30 ps and was assigned to the collective rotational diffusion of the molecules within the sample. The faster relaxation component was omitted from discussion due to high uncertainties associated with its fitting. Indeed, fitting of the two-component model to our liquid mixture gave similar results; in particular, notable fluctuations in the femtosecond component. We have therefore employed a three-component Debye model to analyze the aqueous alcohol mixture data, where τ_1 and τ_2 were constrained to the values of the relaxation times of pure water and the respective pure alcohol (τ_1 of a two-component fit to the terahertz spectra only in Table 1) in order to resolve the relaxation process of the bulk water and bulk alcohol structures within the mixture. The key assumption we make is that the characteristic relaxation times of bulk water and alcohol are identical to the picosecond relaxation times identified using terahertz data only which is justified given we are fitting dielectric spectra of alcohol/water mixture at terahertz frequencies alone. In this context it is important to note that in contrast to previous work in our implementation of the three-component model the first two components do not represent the lifetime of the locally stable molecular configuration in the energy landscape of the liquid and the motion of individual alcohol molecules, respectively;[45] but in our model we constrain these terms by fixing τ_1 and τ_2 to the relaxation behavior of bulk water and alcohol. Furthermore, we would like to highlight that the Debye weight ε_1 of the 2-comonent fit of the terahertz data alone and the sum of the Debye weights $\varepsilon_1 + \varepsilon_2$ of the three-component Debye fit to the combined terahertz and gigahertz spectra match very well (methanol: 29.03/29.28 ps; ethanol: 21.75/21.48 ps; 1-propanol: 17.81/17.66 ps; and 2-propanol: 16.90/16.66 ps) further justifying the validity of our methodology. The parameters ε_1, ε_2, ε_3, and τ_3 are free variables where the relaxation strengths ε_1 and ε_2 are assumed to represent the relative number of molecules present within the respective liquid structural domains.

The results of the fits are shown in Figure 5. In all cases the relaxation strengths of the femtosecond term are extremely small. We therefore focus discussion on the behavior of the two picosecond terms.
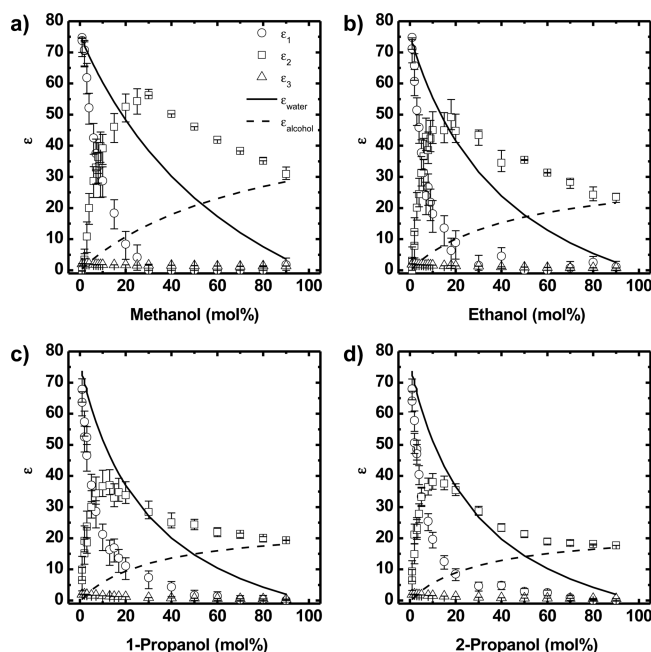

Figure 5. Relaxation strengths of alcohol/water mixtures evaluated by three-component Debye model: ε_1, ε_2, and ε_3 and ideal values ε_{water} and $\varepsilon_{alcohol}$ calculated according to eq 6 for different alcohol/water mixtures: (a) methanol/water mixtures; (b) ethanol/water mixtures; (c) 1-propanol/water mixtures; (d) 2-propanol/water mixtures. Error bars were calculated from the average values of the extracted parameters by fitting the same model to multiple experimental data sets that were measured independently.

Also shown in Figure 5 are the calculated theoretical relaxation strengths of bulk water (ε_{water}) and bulk alcohol structures ($\varepsilon_{alcohol}$) based on an ideal mixing model. Under such conditions, all liquid molecules preserve their rotational dynamics as if they were part of a pure water or pure alcohol sample. Consequently, the corresponding dielectric relaxation strengths are proportional to their volume fractions:[71−73]

$$\varepsilon_{liquid} = \varepsilon_0 V_{liquid} \tag{7}$$

where ε_0 is the picosecond relaxation strength measured for pure water or pure alcohols using the two-component Debye model. V_{liquid} is the volume fraction of the liquid at a given concentration of the mixture; ε_{liquid} is the relaxation strength of the corresponding bulk liquid structure in an ideal mixture; ε_{water} and $\varepsilon_{alcohol}$, as calculated according to eq 7 are plotted in Figure 5 as solid and dashed lines, respectively. Compared to the experimental values of ε_1, the theoretical values of ε_{water} are larger over the entire concentration range of the mixtures. This decrease in ε in the real mixture is consistent with the disruption of the water structure by alcohol molecules. In contrast, the extracted values of ε_2 are higher than the ideal values $\varepsilon_{alcohol}$. This result is unphysical as the ideal values $\varepsilon_{alcohol}$ define the upper limit of possible dielectric constant of bulk alcohol structure; we assume all alcohol molecules are part of bulk alcohol structure in an ideal model. Hence, the extracted values ε_2 must include contributions from other relaxation

10161

dx.doi.org/10.1021/jp502799x | *J. Phys. Chem. B* 2014, 118, 10156−10166

processes. Previous reports indicate three possible bulk structures form in the alcohol/water mixtures:[7,52,58,59,74] (i) an extended water structure; (ii) an extended alcohol structure, which contain only water or alcohol molecules respectively; and (iii) an extended hydrogen bonded alcohol/water network. Considering the extreme case where there is only a single alcohol molecule in water, the mixture would be dominated by the extended water structure and the majority of water molecules would not be affected by the presence of the single alcohol molecule. Therefore, the relaxation time of this bulk water structure remains indistinguishable from that of pure water (~7 ps). Following the same logic, an extended alcohol structure also exists in alcohol-rich mixtures with relaxation times similar to that of the pure alcohol (~picosecond range with values of τ_1 in Table 1). It is the extended hydrogen-bonded alcohol/water network that is responsible for the overall slow-down of the rotational dynamics of alcohol/water mixtures that is observed at terahertz frequencies. However, as outlined above the relaxation times of alcohol/water mixtures fitted by a conventional two-component Debye model in the THz range only predict a single picosecond component which varies with concentration, since this model is not capable of differentiating between multiple picosecond relaxation processes within the mixture. The predicted picosecond relaxation time is therefore effectively the weighted average of the above three bulk structures if they exist in the mixture. As we have already discussed, if ε_1 represents bulk water, then we can conclude that ε_2 most likely represents bulk alcohol and alcohol−water structures (this is validated in the Discussion, where we compare results shown in Figure 5 with relative absorption measurement, Figure 3). Inspection of Figure 5 shows that the maximum in ε_2 and the maximum difference between ε_2 and $\varepsilon_{\text{alcohol}}$ is observed at alcohol concentrations of approximately 30, 15, 10, and 10 mol % for methanol, ethanol, 1-propanol, and 2-propanol aqueous mixtures, respectively.

It is also seen in Figure 5 that the relaxation strength of water decreases to zero as the mole fraction of alcohol increases. We now use these data to estimate the number of water molecules around an individual alcohol molecule in the water-rich region of the binary mixture. This estimate of the size of the hydration shell that is formed around alcohol molecules is obtained based on the number ratio N between water and alcohol molecules in the hydrogen bonded alcohol/water network. The value of N is calculated as

$$n_{\text{bulk-water}} = \frac{\varepsilon_1 n_0}{\varepsilon_0} \tag{8}$$

$$N = \frac{n_{\text{HB,water}}}{n_{\text{HB,alcohol}}} = \frac{n_{\text{water}} - n_{\text{bulk-water}}}{n_{\text{alcohol}}} \tag{9}$$

where n_0 is the number of water molecules per unit volume in pure water and ε_0 the relaxation strength; n_{water} and n_{alcohol} are the total number of liquid molecules per unit volume in the mixture at an alcohol concentration of x_a, while $n_{\text{HB,water}}$ and $n_{\text{HB,alcohol}}$ are the number of hydrogen-bonded liquid molecules per unit volume in the mixture at x_a; ε_1 is the dielectric relaxation strength of bulk water structure extracted from the constrained three-component Debye model. The relaxation strength is assumed to be linearly proportional to the number of corresponding liquid molecules.[57,71−73] In this calculation, we omit the free liquid molecules in the mixtures as their number is negligible. At the same time, $n_{\text{HB,alcohol}} \approx n_{\text{alcohol}}$

because there is no bulk alcohol structure in the water-rich region as noted before.

Figure 6 shows the results of this analysis. At the lowest mole fractions of alcohol studied a relatively constant value of N is
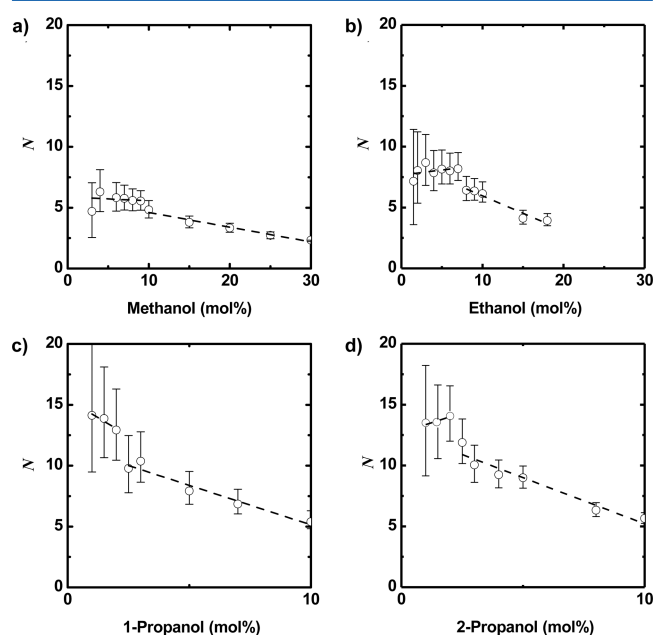

Figure 6. Number ratio, N, which represents the extent of hydration shell, between water and alcohol molecules in the hydrogen-bonded networks for the range of $x_a < x_2$ in different alcohol/water mixtures: (a) methanol/water; (b) ethanol/water; (c) 1-propanol/water; (d) 2-propanol/water. The dashed and dotted lines were plotted to guide the eye. The error bars are derived from the errors in ε_1 (Figure 5).

obtained. Upon increasing the alcohol mole fraction beyond a critical concentration, x_1, the value of N decreases. x_1 takes the value 10 ± 2, 7 ± 2, 2 ± 1, and 2 ± 1 mol % for methanol, ethanol, 1-propanol, and 2-propanol, respectively. We interpret these results as being due to independent hydration shells of N water molecules existing up to a mole fraction of alcohol x_1, after which independent hydration shells can no longer be maintained due to the increasing number of alcohol molecules in the mixtures. This leads to a steady decrease in N, which is the averaged number ratio between alcohol and water molecules in the entire hydrogen bonded alcohol/water network. The values of N determined from Figure 6 are 5.6 ± 1.3, 8.0 ± 2.0, 13.6 ± 3.6, and 13.7 ± 3.3, respectively.

In summary, alcohol molecules with larger hydrophobic moieties form larger hydration shells and the concentration at which these hydration shells start to overlap is lower. This indicates the important role of the hydrophobic moiety of alcohol molecules on determining the structures of alcohol/water mixtures, which has been reported by various techniques such as thermodynamic measurements,[75] NMR,[12] and microwave dielectric spectroscopy.[50]

Diffusion Coefficients of Alcohol and Water Molecules in the Mixture. The self-diffusion coefficients of various alcohol/water mixtures were measured by PFG-NMR across the entire composition range and the data are shown in Figure 7. The data are largely consistent with those reported by Price et al.[68] for aqueous methanol, ethanol and *tert*-butyl alcohol solutions. Previous theoretical and experimental measurements, utilizing a magnetically stirred diaphragm cell, of the self-
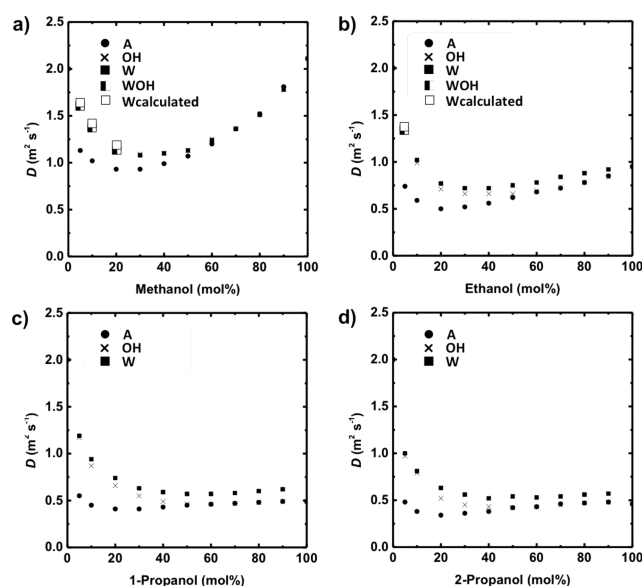
Figure 7. Self-diffusion coefficients of water (W), hydroxyl groups (OH), and alkyl groups (A) in different alcohol/water mixtures: (a) methanol/water mixtures; (b) ethanol/water mixtures; (c) 1-propanol/water mixtures; (d) 2-propanol/water mixtures. WOH refers to the combined diffusion coefficient of the water and alcohol −OH NMR peak (as their respective single peaks overlap at low mole fractions in ethanol, below 5% mole fraction, and methanol mixtures, below 20% mole fraction; symbols for these compositions are enlarged to facilitate the identification). Wcalculated is the diffusion coefficient of water calculated according to eq 2 in ref 68. In methanol/water mixtures the hydroxyl resonance of methanol has a self-diffusivity value similar to water over the whole composition range.

diffusion coefficients of water and methanol/ethanol in aqueous alcohol solutions also show good agreement with the data from PFG-NMR acquired in this study.[21,76]

Three spectral resonances are identified in the ^{1}H PFG-NMR data corresponding to the ^{1}H species associated with the alkyl chain of the alcohol, the OH group of the alcohol and the water molecules; the diffusion coefficients that are determined from these data are referred to as D_A, D_{OH}, and D_W, respectively. When ^{1}H fast exchange occurs (i.e., fast proton exchange) the spectral resonance frequencies of the OH and water ^{1}H species take an average value and are associated with a single resonance frequency. This behavior is observed in the case of methanol/water and ethanol/water mixtures. This single value of diffusivity is identified as D_{WOH}. Under these conditions the diffusion coefficient of the water and the alcohol OH will be approximately the same.[68] Our measurements are carried out at 293 K. At this temperature, we observed fast proton exchange between methanol and water to concentrations up to 20% mole fraction of methanol. The diffusion coefficient of water, $D_{Wcalculated}$, was calculated according to the method introduced by Price at al. and is almost identical to the diffusion coefficient of the single hydroxyl resonance representative of the fast proton exchange between alcohol and water D_{WOH}. At mole fractions greater than 20%, the alcohol OH and water resonances become distinguishable and it is possible to measure unambiguously the diffusion coefficient of both species; that is, D_{OH} and D_W. For the ethanol−water mixture, fast proton exchange between the alcohol and water occurs up to 5% mole fraction. In aqueous mixtures of 1-propanol and 2-propanol, no fast exchange is observed, at least down to the lowest mole

fraction studied here (5%). It is noted that Price et al.[68] reported very similar behavior. However, in methanol/water mixtures they observed fast exchange up to 40% mole fraction of alcohol; in ethanol/water, the fast exchange was observed up to 20% mole fraction of alcohol. These values are higher than those observed in this work and may be due to the fact that our measurements are carried out at a lower temperature than that used in their experiments.

Starting from an alcohol mole fraction $x_a = 0$, the self-diffusion coefficients of all the species decrease sharply, reaching a minimum and then increasing again but in a less pronounced way (Figure 6). A lag in the decrease of D_A and D_W is observed, with D_A reaching a minimum at a lower mole fraction. Moreover, at lower alcohol mole fractions D_{OH} is similar to D_W; however, as x_a increases D_{OH} tends to the value of D_A. Above a certain mole fraction $D_A = D_{OH}$ to within the accuracy of the measurement. The value of composition at which this occurs is 70% for methanol/water, 60% for ethanol/water, and 50% for 1-propanol/water and 2-propanol/water. It has to be noted that in the case of methanol/water mixtures $D_W \cong D_{OH}$ throughout the whole composition range.

■ DISCUSSION

The rapid decrease of water and alcohol self-diffusion coefficients in the water-rich region (see Figure 7) indicates that there is an increasing intermolecular interaction between alcohol and water molecules. This observation was also reported by Price et al.[68] The fact that the self-diffusivity of the alcohol is reaching a minimum before a minimum is observed for the self-diffusivity of water implies the formation of hydration structures around the alcohol molecules. The number of water molecules involved in the formation of stable hydration shell depends on the alcohol mole fraction and as this increases, it reaches a point where insufficient water molecules remain to form stable hydration shells.[68] The estimates of the hydration shell dimensions obtained from the terahertz measurements (Figure 6) provide an independent validation of this hypothesis as we indeed observe that the size of these hydration structures decreases as the alcohol mole fraction increases. Moreover, the results also give us more detailed information on these structures. Figure 6 shows that larger hydration shells are formed around alcohol molecules with larger hydrophobic moieties. This clearly demonstrates the effect of the hydrophobic moiety on the structuring of alcohol/water mixtures. At this point it is interesting to note that it has previously been observed that alcohols with larger and more sterically hindering groups favor the stabilization of more water molecules in the hydrophobic hydration shells.[68] Measurements of [17]O spin−lattice relaxation time have yielded estimates of the dynamic hydration numbers of coordinating water molecules around mono- and diols.[11] Values of 5.8, 10.5, 14.1, and 16.4 were reported for methanol, ethanol, 1-propanol, and 2-propanol, respectively. These compare with values of N obtained in the present work of 5.6 ± 1.3, 8.0 ± 2.0, 13.6 ± 3.6, and 13.7 ± 3.3. Based on a fs-IR spectroscopy study Rezus and Bakker[8] reported a linear correlation between the number of dynamically retarded water molecules in the solvation shell around biologically relevant molecules and the number of methyl groups in the solute molecule at low solute mole fractions. The obtained value of ~4 water molecules per alkyl(ene) group also agrees well with the values of N reported herein for aliphatic alcohols and our results are also in good agreement with other dielectric studies that cover terahertz

frequencies.[61] It is noted that the size of the hydration shells N_0 reported here and these other experimental studies is systematically larger than the average number of hydrogen bonds per liquid molecule that was previously calculated using MD simulations.[7,74,77] This suggests that the alcohol molecules must affect water molecules beyond the first coordination shell, which can also be considered as an implication of the hydrophobic effect and again corroborates the results presented by Tielrooij et al.[61] The mole fraction at which these hydration shells become less well structured is 10% for methanol, 7% for ethanol, approximately 2% for 1-propanol and 2-propanol. Above these values of mole fraction, hydration structures become less stable and there is a preference for water to aggregate around the −OH of the alcohol,[68] hence, favoring the formation of extended hydrogen bonds rather than forming hydrophobic hydration shells through interactions with the aliphatic group.

By inspection of Figure 4, the excess values of ε_2 compared to $\varepsilon_{alcohol}$ can indeed be explained by the presence of an extended hydrogen-bonded alcohol/water network that forms in the mixtures of alcohol and water.[7,52,58,59,74] The difference $\varepsilon_2 - \varepsilon_{alcohol}$ represents the extent of hydrogen-bonded alcohol/water networks in various alcohol/water mixtures. The highest degree of structuring, that is, the highest difference between ε_2 and $\varepsilon_{alcohol}$, occurs at mole fractions of approximately 30% for methanol, 15% for ethanol, and 10% 1-propanol and 2-propanol aqueous mixtures, respectively. Considering the errors on both the values in Figure 5 and those in Figure 7, these values of mole fractions are close to those at which a minimum in alcohol self-diffusion coefficient occurs (see Figure 6) and this suggests that the highest degree of structuring in the hydrogen bonded alcohol/water network is responsible for the lowest translational dynamics observed, that is, the diffusion behavior of the alcohol is dominated by hydrogen bonding interactions. The mole fraction at which the maximum difference between ε_2 and $\varepsilon_{alcohol}$ occurs is approximately the same at which the maximum in α_{real} is observed (see Figure 3), which, again, indicates the formation of extended hydrogen boding with slower dynamics.[58,60]

Another critical mole fraction is that at which the self-diffusion coefficient of the −OH group of the alcohol becomes equal to that of the aliphatic group (i.e., $D_{OH} = D_A$). This occurs at 70% mole fraction for methanol, 60% for ethanol, and 50% for 1-propanol and 2-propanol. Above this alcohol mole fraction, the diffusion rate of both hydroxyl and alkyl group of the alcohol is essentially the same. This observation suggests that at higher alcohol mole fractions the solution dynamics of water and alcohol molecules become increasingly independent, in agreement with that reported by PGSE studies of Price et al.[68] There is suggestion of an inflection point in the terahertz (α_{real}) at similar mole fractions (see Figure 3). However, more accurate terahertz data are required to confirm this.

In summary, starting from an alcohol mole fraction $x_a = 0$, we can identify the following critical mole fractions that describes the dynamics of these alcohol/water mixtures:

(i) x_1 identifies the concentration above which intermolecular interactions between water and the alcohol −OH become predominant as compared to hydrophobic hydration interactions (see Figure 6).

(ii) Above this mole fraction these hydrophobic hydration structures become less stable and there is a preference for water to aggregate around the −OH of the alcohol, forming extended hydrogen bonding networks.

(iii) The highest degree of structuring of such a network is reached at a mole fraction x_2, which is identified by the maximum difference in $\varepsilon_2 - \varepsilon_{alcohol}$ (Figure 5), which also corresponds to the maximum value of α_{real} (Figure 3). This is also the composition at which there is a minimum in the diffusivity of alcohol in the various alcohol/water mixtures, as shown in Figure 7.

(iv) Finally, x_3 identifies the composition at which the solution dynamics of water and alcohol molecules becomes increasingly independent, which corresponds to the merging point of D_A and D_{OH} of the alcohol (see Figure 7).

CONCLUSIONS

Terahertz spectroscopy and PFG-NMR diffusometry have been used as complementary techniques to understand the dynamics of alcohol/water mixtures at the molecular level. Terahertz measurements were performed to measure absorption coefficients of the various alcohol/water mixtures at different compositions and to calculate relaxation strength and dielectric relaxation constants. The PFG-NMR method was then used to investigate molecular diffusivity of these systems. The combined results show the presence of three critical concentrations at which a change in the dynamic regime occurs: x_1, the concentration above which intermolecular interactions between water and the alcohol −OH become predominant when compared to hydrophobic hydration interactions. Below this composition, hydration shells around the hydrophobic moieties of the alcohols form predominantly, with larger hydrophobic moieties of the alcohol molecule resulting in larger hydration shells. At a higher concentration, x_2, the highest degree of structuring of the hydrogen bonded network occurs, which corresponds to the slowest translational dynamics within the mixture. Finally, at a concentration of, x_3, the dynamics of water and alcohol molecules become increasingly independent. Each of these transition points were identified by specific signatures in the profiles of terahertz and PFG-NMR measurements. This work highlights the differences in mesoscopic structure for liquid solutions that appear homogeneous on a macroscopic length scale, which may have significant implication in technological application, such as catalytic reactions in liquid phase and separation processes.

ASSOCIATED CONTENT

Ⓢ Supporting Information

The terahertz absorption spectra of methanol/water, ethanol/water, 1-propanol/water, and 2-propanol/water over a range of concentrations are presented in the associated content. This material is available free of charge via the Internet at http://pubs.acs.org.

AUTHOR INFORMATION

Corresponding Authors
*E-mail: jaz22@cam.ac.uk. Tel.: +44 (0)1223 (3)34762.
*E-mail: lfg1@cam.ac.uk.

Present Address
†Department of Chemical and Biological Engineering, University of Sheffield, Mappin Street, Sheffield S1 3JD, U.K. (J.M.).

◾ REFERENCES

(1) Akpa, B. S.; D'Agostino, C.; Gladden, L. F.; Hindle, K.; Manyar, H.; McGregor, J.; Li, R.; Neurock, M.; Sinha, N.; Stitt, E. H.; et al. Solvent Effects in the Hydrogenation of 2-Butanone. *J. Catal.* **2012**, *289*, 30−41.

(2) Hilser, V. J. Structural Biology: Finding the Wet Spots. *Nature* **2011**, *469*, 166−167.

(3) Ball, P. Water: Water—an Enduring Mystery. *Nature* **2008**, *452*, 291−292.

(4) Palo, D. R.; Dagle, R. A.; Holladay, J. D. Methanol Steam Reforming for Hydrogen Production. *Chem. Rev.* **2007**, *107*, 3992−4021.

(5) Frank, H. S.; Evans, M. W. Free Volume and Entropy in Condensed Systems III. Entropy in Binary Liquid Mixtures; Partial Molal Entropy in Dilute Solutions; Structure and Thermodynamics in Aqueous Electrolytes. *J. Chem. Phys.* **1945**, *13*, 507.

(6) Dougan, L.; Hargreaves, R.; Bates, S. P.; Finney, J. L.; Réat, V.; Soper, A. K.; Crain, J. Segregation in Aqueous Methanol Enhanced by Cooling and Compression. *J. Chem. Phys.* **2005**, *122*, 174514−174514.

(7) Dixit, S.; Crain, J.; Poon, W.; Finney, J.; Soper, A. Molecular Segregation Observed in a Concentrated Alcohol—Water Solution. *Nature* **2002**, *416*, 829−832.

(8) Rezus, Y. L.; Bakker, H. J. Observation of Immobilized Water Molecules Around Hydrophobic Groups. *Phys. Rev. Lett.* **2007**, *99*, 148301−148301.

(9) Sciortino, F.; Geiger, A.; Stanley, H. E. Effect of Defects on Molecular Mobility in Liquid Water. *Nature* **1991**, *354*, 218−221.

(10) Corsaro, C.; Spooren, J.; Branca, C.; Leone, N.; Broccio, M.; Kim, C.; Chen, S.-H.; Stanley, H. E.; Mallamace, F. Clustering Dynamics in Water/Methanol Mixtures: a Nuclear Magnetic Resonance Study at 205 K. *J. Phys. Chem. B* **2008**, *112*, 10449−10454.

(11) Ishihara, Y.; Okouchi, S.; Uedaira, H. Dynamics of Hydration of Alcohols and Diols in Aqueous Solutions. *J. Chem. Soc., Faraday Trans.* **1997**, *93*, 3337−3342.

(12) Coccia, A.; Indovina, P. L.; Podo, F.; Viti, V. PMR Studies on the Structures of Water—Ethyl Alcohol Mixtures. *Chem. Phys.* **1975**, *7*, 30−40.

(13) Lin, K.; Hu, N.; Zhou, X.; Liu, S.; Luo, Y. Reorientation Dynamics in Liquid Alcohols From Raman Spectroscopy. *J. Raman Spectrosc.* **2012**, *43*, 82−88.

(14) Nedić, M.; Wassermann, T. N.; Larsen, R. W.; Suhm, M. A. A Combined Raman- and Infrared Jet Study of Mixed Methanol—Water and Ethanol—Water Clusters. *Phys. Chem. Chem. Phys.* **2011**, *13*, 14050−14063.

(15) Nishi, N.; Takahashi, S.; Matsumoto, M.; Tanaka, A.; Muraya, K.; Takamuku, T.; Yamaguchi, T. Hydrogen-Bonded Cluster Formation and Hydrophobic Solute Association in Aqueous Solutions of Ethanol. *J. Phys. Chem.* **1995**, *99*, 462−468.

(16) Sato, T.; Chiba, A.; Nozaki, R. Dynamical Aspects of Mixing Schemes in Ethanol—Water Mixtures in Terms of the Excess Partial Molar Activation Free Energy, Enthalpy, and Entropy of the Dielectric Relaxation Process. *J. Chem. Phys.* **1999**, *110*, 2508.

(17) Wakisaka, A.; Matsuura, K.; Uranaga, M.; Sekimoto, T.; Takahashi, M. Azeotropy of Alcohol—Water Mixtures From the Viewpoint of Cluster-Level Structures. *J. Mol. Liq.* **2011**, *160*, 103−108.

(18) Mejía, S. M.; Flórez, E.; Mondragón, F. An Orbital and Electron Density Analysis of Weak Interactions in Ethanol—Water, Methanol—Water, Ethanol and Methanol Small Clusters. *J. Chem. Phys.* **2012**, *136*, 144306.

(19) Biscay, F.; Ghoufi, A.; Malfreyt, P. Surface Tension of Water—Alcohol Mixtures From Monte Carlo Simulations. *J. Chem. Phys.* **2011**, *134*, 044709−044709.

(20) Marcus, Y. Water Structure Enhancement in Water-Rich Binary Solvent Mixtures. Part II. the Excess Partial Molar Heat Capacity of the Water. *J. Mol. Liq.* **2012**, *166*, 62−66.

(21) Guevara-Carrion, G.; Vrabec, J.; Hasse, H. Prediction of Self-Diffusion Coefficient and Shear Viscosity of Water and Its Binary Mixtures with Methanol and Ethanol by Molecular Simulation. *J. Chem. Phys.* **2011**, *134*, 074508.

(22) Dolenko, T. A.; Burikov, S. A.; Patsaeva, S. V.; Yuzhakov, V. I. Manifestation of Hydrogen Bonds of Aqueous Ethanol Solutions in the Raman Scattering Spectra. *Quantum Electron.* **2011**, *41*, 267−272.

(23) Larkin, J. A. Thermodynamic Properties of Aqueous Non-Electrolyte Mixtures I. Excess Enthalpy for Water + Ethanol at 298.15 to 383.15 K. *J. Chem. Thermodyn.* **1975**, *7*, 137−148.

(24) Towey, J. J.; Dougan, L. Structural Examination of the Impact of Glycerol on Water Structure. *J. Phys. Chem. B* **2012**, *116*, 1633−1641.

(25) Towey, J. J.; Soper, A. K.; Dougan, L. Preference for Isolated Water Molecules in a Concentrated Glycerol—Water Mixture. *J. Phys. Chem. B* **2011**, *115*, 7799−7807.

(26) Vanexter, M.; Fattinger, C.; Grischkowsky, D. R. Terahertz Time-Domain Spectroscopy of Water Vapor. *Opt. Lett.* **1989**, *14*, 1128−1130.

(27) Schmuttenmaer, C. Exploring Dynamics in the Far-Infrared with Terahertz Spectroscopy. *Chem. Rev.* **2004**, *104*, 1759−1779.

(28) Walther, M.; Fischer, B.; Schall, M.; Helm, H.; Jepsen, P. Far-Infrared Vibrational Spectra of All-Trans, 9-Cis and 13-Cis Retinal Measured by THz Time-Domain Spectroscopy. *Chem. Phys. Lett.* **2000**, *332*, 389−395.

(29) Zeitler, J. A.; Taday, P. F.; Pepper, M.; Rades, T. Relaxation and Crystallization of Amorphous Carbamazepine Studied by Terahertz Pulsed Spectroscopy. *J. Pharm. Sci.* **2007**, *96*, 2703−2709.

(30) Zeitler, J. A.; Taday, P. F.; Gordon, K. C.; Pepper, M.; Rades, T. Solid-State Transition Mechanism in Carbamazepine Polymorphs by Time-Resolved Terahertz Spectroscopy. *ChemPhysChem* **2007**, *8*, 1924−1927.

(31) Tonouchi, M. Cutting-Edge Terahertz Technology. *Nat. Photonics* **2007**, *1*, 97−105.

(32) Li, R.; Zeitler, J. A.; Tomerini, D.; Parrott, E. P. J.; Gladden, L. F.; Day, G. A Study Into the Effect of Subtle Structural Details and Disorder on the Terahertz Spectrum of Crystalline Benzoic Acid. *Phys. Chem. Chem. Phys.* **2010**, *12*, 5329−5340.

(33) Takahashi, M.; Kawazoe, Y.; Ishikawa, Y.; Ito, H. Interpretation of Temperature-Dependent Low Frequency Vibrational Spectrum of Solid-State Benzoic Acid Dimer. *Chem. Phys. Lett.* **2009**, *479*, 211−217.

(34) Allis, D.; Prokhorova, D.; Korter, T. Solid-State Modeling of the Terahertz Spectrum of the High Explosive HMX. *J. Phys. Chem. A* **2006**, *110*, 1951−1959.

(35) Grischkowsky, D. R.; Keiding, S.; Vanexter, M.; Fattinger, C. Far-Infrared Time-Domain Spectroscopy with Terahertz Beams of Dielectrics and Semiconductors. *J. Opt. Soc. Am. B* **1990**, *7*, 2006−2015.

(36) Naftaly, M.; Miles, R. Terahertz Time-Domain Spectroscopy of Silicate Glasses and the Relationship to Material Properties. *J. Appl. Phys.* **2007**, *102*, 043517.

(37) Taraskin, S. N.; Simdyankin, S.; Elliott, S.; Neilson, J.; Lo, T. Universal Features of Terahertz Absorption in Disordered Materails. *Phys. Rev. Lett.* **2006**, *97*, 055504.

(38) Duvillaret, L.; Garet, F.; Coutaz, J. L. Highly Precise Determination of Optical Constants and Sample Thickness in Terahertz Time-Domain Spectroscopy. *Appl. Opt.* **1999**, *38*, 409−415.

(39) Pupeza, I.; Wilk, R.; Koch, M. Highly Accurate Optical Material Parameter Determination with THz Time-Domain Spectroscopy. *Opt. Express* **2007**, *15*, 4335−4350.

(40) Parrott, E. P. J.; Zeitler, J. A.; Gladden, L. F.; Taraskin, S. N.; Elliott, S. Extracting Accurate Optical Parameters From Glasses Using

10165

dx.doi.org/10.1021/jp502799x | *J. Phys. Chem. B* 2014, 118, 10156−10166

Terahertz Time-Domain Spectroscopy. *J. Non-Cryst. Solids* **2009**, *355*, 1824−1827.

(41) Sibik, J.; Shalaev, E. Y.; Zeitler, J. A. Glassy Dynamics of Sorbitol Solutions at Terahertz Frequencies. *Phys. Chem. Chem. Phys.* **2013**, *15*, 11931−11942.

(42) Sibik, J.; Elliot, S. R.; Zeitler, J. A. Thermal Decoupling of Molecular-Relaxation Processes From the Vibrational Density of States at Terahertz Frequencies in Supercooled Hydrogen-Bonded Liquids. *J. Phys. Chem. Lett.* **2014**, 1968−1972.

(43) Barthel, J.; Bachhuber, K.; Buchner, R.; Hetzenauer, H. Dielectric Spectra of Some Common Solvents in the Microwave Region. Water and Lower Alcohols. *Chem. Phys. Lett.* **1990**, *165*, 369−373.

(44) Bertolini, D.; Cassettari, M.; Salvetti, G.; Tombari, E. Dielectric Relaxation of Water−Alcohol and Alcohol−Alcohol Solutions. *J. Non-Cryst. Solids* **1991**, *131−133*, 1169−1173.

(45) Sato, T.; Buchner, R. Dielectric Relaxation Spectroscopy of 2-Propanol−Water Mixtures. *J. Chem. Phys.* **2003**, *118*, 4606−4613.

(46) Sato, T.; Buchner, R. Cooperative and Molecular Dynamics of Alcohol/Water Mixtures: the View of Dielectric Spectroscopy. *J. Mol. Liq.* **2005**, *117*, 23−31.

(47) Sato, T.; Buchner, R. The Cooperative Dynamics of the H-Bond System in 2-Propanol/Water Mixtures: Steric Hindrance Effects of Nonpolar Head Group. *J. Chem. Phys.* **2003**, *119*, 10789−10800.

(48) Sato, T.; Buchner, R. Dielectric Relaxation Processes in Ethanol/Water Mixtures. *J. Phys. Chem. A* **2004**, *108*, 5007−5015.

(49) Sato, T.; Buchner, R. Cooperative and Molecular Dynamics of Alcohol/Water Mixtures: the View of Dielectric Spectroscopy. *J. Mol. Liq.* **2005**, *117*, 23−31.

(50) Sato, T.; Chiba, A.; Nozaki, R. Hydrophobic Hydration and Molecular Association in Methanol−Water Mixtures Studied by Microwave Dielectric Analysis. *J. Chem. Phys.* **2000**, *112*, 2924.

(51) Sato, T.; Chiba, A.; Nozaki, R. Composition-Dependent Dynamical Structures of 1-Propanol−Water Mixtures Determined by Dynamical Dielectric Properties. *J. Chem. Phys.* **2000**, *113*, 9748.

(52) Sato, T.; Chiba, A.; Nozaki, R. Dielectric Relaxation Mechanism and Dynamical Structures of the Alcohol/Water Mixtures. *J. Mol. Liq.* **2002**, *101*, 99−111.

(53) Sato, T.; Chiba, A.; Nozaki, R. Composition-Dependent Dynamical Structures of Monohydric Alcohol−Water Mixtures Studied by Microwave Dielectric Analysis. *J. Mol. Liq.* **2002**, *96−7*, 327−339.

(54) Barthel, J. M. G.; Buchner, R. High Frequency Permittivity and Its Use in the Investigation of Solution Properties. *Pure Appl. Chem.* **1991**, *63*, 1473−1482.

(55) Ronne, C.; Thrane, L.; Astrand, P.; Wallqvist, A.; Mikkelsen, K.; Keiding, S. Investigation of the Temperature Dependence of Dielectric Relaxation in Liquid Water by THz Reflection Spectroscopy and Molecular Dynamics Simulation. *J. Chem. Phys.* **1997**, *107*, 5319−5331.

(56) Schmidt, D. A.; Birer, O.; Funkner, S.; Born, B. P.; Gnanasekaran, R.; Schwaab, G. W.; Leitner, D. M.; Havenith, M. Rattling in the Cage: Ions as Probes of Sub-Picosecond Water Network Dynamics. *J. Am. Chem. Soc.* **2009**, *131*, 18512−18517.

(57) Tielrooij, K. J.; Paparo, D.; Piatkowski, L.; Bakker, H. J.; Bonn, M. Dielectric Relaxation Dynamics of Water in Model Membranes Probed by Terahertz Spectroscopy. *Biophys. J.* **2009**, *97*, 2484−2492.

(58) Venables, D.; Schmuttenmaer, C. Spectroscopy and Dynamics of Mixtures of Water with Acetone, Acetonitrile, and Methanol. *J. Chem. Phys.* **2000**, *113*, 11222−11236.

(59) Yada, H.; Nagai, M.; Tanaka, K. Origin of the Fast Relaxation Component of Water and Heavy Water Revealed by Terahertz Time-Domain Attenuated Total Reflection Spectroscopy. *Chem. Phys. Lett.* **2008**, *464*, 166−170.

(60) Venables, D.; Schmuttenmaer, C. Far-Infrared Spectra and Associated Dynamics in Acetonitrile-Water Mixtures Measured with Femtosecond THz Pulse Spectroscopy. *J. Chem. Phys.* **1998**, *108*, 4935−4944.

(61) Tielrooij, K.-J.; Hunger, J.; Buchner, R.; Bonn, M.; Bakker, H. J. Influence of Concentration and Temperature on the Dynamics of Water in the Hydrophobic Hydration Shell of Tetramethylurea. *J. Am. Chem. Soc.* **2010**, *132*, 15671−15678.

(62) Hu, N.; Wu, D.; Cross, K. J.; Schaefer, D. W. Structural Basis of the ^{1}H-Nuclear Magnetic Resonance Spectra of Ethanol−Water Solutions Based on Multivariate Curve Resolution Analysis of Mid-Infrared Spectra. *Appl. Spectrosc.* **2010**, *64*, 337−342.

(63) Mizuno, K.; Miyashita, Y.; Shindo, Y.; Ogawa, H. NMR and FT-IR Studies of Hydrogen Bonds in Ethanol−Water Mixtures. *J. Phys. Chem.* **1995**, *99*, 3225−3228.

(64) Luz, Z.; Gill, D.; Meiboom, S. NMR Study of the Protolysis Kinetics in Methanol and Ethanol. *J. Chem. Phys.* **1959**, *30*, 1540.

(65) Arnold, J. Magnetic Resonances of Protons in Ethyl Alcohol. *Phys. Rev.* **1956**, *102*, 136−150.

(66) Corsaro, C.; Spooren, J.; Branca, C.; Leone, N.; Broccio, M.; Kim, C.; Chen, S.-H.; Stanley, H. E.; Mallamace, F. Clustering Dynamics in Water/Methanol Mixtures: a Nuclear Magnetic Resonance Study at 205 K. *J. Phys. Chem. B* **2008**, *112*, 10449−10454.

(67) Yoshida, K.; Kitajo, A.; Yamaguchi, T. ^{17}O NMR Relaxation Study of Dynamics of Water Molecules in Aqueous Mixtures of Methanol, Ethanol, and 1-Propanol Over a Temperature Range of 283−403 K. *J. Mol. Liq.* **2006**, *125*, 158−163.

(68) Price, W. S.; Ide, H.; Arata, Y. Solution Dynamics in Aqueous Monohydric Alcohol Systems. *J. Phys. Chem. A* **2003**, *107*, 4784−4789.

(69) Tanner, J. E. Use of the Stimulated Echo in NMR Diffusion Studies. *J. Chem. Phys.* **1970**, *52*, 2523.

(70) Paterson, W. G. Nuclear Magnetic Resonance Measurements Of Proton Exchange In Alcohol−Water Systems: Part II N-C$_3$H$_7$OH−H$_2$O and I-C$_3$H$_7$OH−H$_2$O. *Can. J. Chem.* **1963**, *41*, 2472−2476.

(71) Miura, N.; Shioya, S.; Kurita, D.; Shigematsu, T.; Mashimo, S. Time Domain Reflectometry: Measurement of Free Water in Normal Lung and Pulmonary Edema. *Am. J. Physiol.* **1999**, *276*, 207−212.

(72) Miura, N.; Yagihara, S.; Mashimo, S. Microwave Dielectric Properties of Solid and Liquid Foods Investigated by Time-Domain Reflectometry. *J. Food Sci.* **2003**, *68*, 1396−1403.

(73) Hayashi, Y.; Katsumoto, Y.; Omori, S.; Kishii, N.; Yasuda, A. Liquid Structure of the Urea−Water System Studied by Dielectric Spectroscopy. *J. Phys. Chem. B* **2007**, *111*, 1076−1080.

(74) Dixit, S.; Soper, A. K.; Finney, J. L.; Crain, J. Water Structure and Solute Association in Dilute Aqueous Methanol. *Europhys. Lett.* **2002**, *59*, 377−383.

(75) Koga, Y.; Nishikawa, K.; Westh, P. Icebergs" or No 'Icebergs' in Aqueous Alcohols?: Composition-Dependent Mixing Schemes. *J. Phys. Chem. A* **2004**, *108*, 3873−3877.

(76) Derlacki, Z. J.; Easteal, A. J.; Edge, A. V. J.; Woolf, L. A.; Roksandic, Z. Diffusion Coefficients of Methanol and Water and the Mutual Diffusion Coefficient in Methanol−Water Solutions at 278 and 298 K. *J. Phys. Chem.* **1985**, *89*, 5318−5322.

(77) Noskov, S. Y.; Lamoureux, G.; Roux, B. Molecular Dynamics Study of Hydration in Ethanol−Water Mixtures Using a Polarizable Force Field. *J. Phys. Chem. B* **2005**, *109*, 6705−6713.

10166

dx.doi.org/10.1021/jp502799x | *J. Phys. Chem. B* 2014, 118, 10156−10166